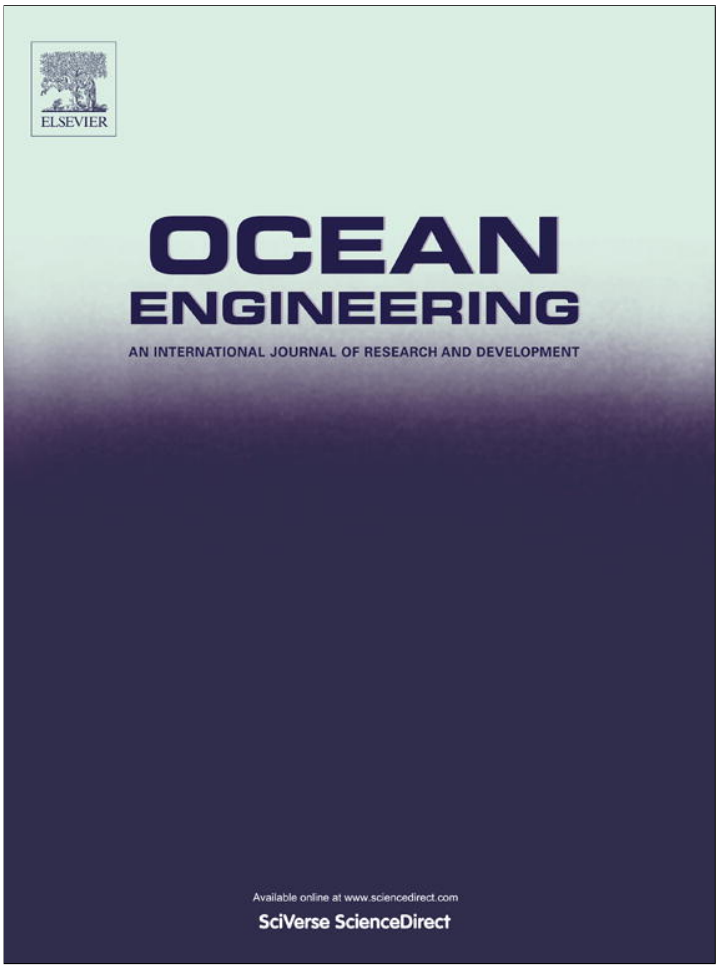


(This is a sample cover image for this issue. The actual cover is not yet available at this time.)

Ocean Engineering 55 (2012) 175–183

Contents lists available at SciVerse ScienceDirect

Ocean Engineering

journal homepage: www.elsevier.com/locate/oceaneng

# Three-mode pneumatic management of marine U-tank systems

Francesco Sorge *, Stefano Beccari, Marco Cammalleri, Giuseppe Genchi, Emiliano Pipitone

*Dipartimento di Ingegneria Chimica, Gestionale, Informatica, Meccanica, Università di Palermo, 90128–Palermo, Italy*

ARTICLE INFO

*Article history:*
Received 9 November 2011
Accepted 28 July 2012

*Keywords:*
U-tank stabilizer
Active operation
Stability control
Optimization

ABSTRACT

This paper deals with a new pneumatic control strategy for the roll damping enhancement of marine U-tank stabilizers. The proposed technique consists in a three-mode operation, where the control is active only within a limited resonant range around the ship natural frequency, whereas the control valves are kept closed in the remaining frequency range. Moreover the connection valve between the two air chambers is either closed or partially opened for the low or high frequencies, respectively. The pressurized air for the active control is fed by a turbo-blower set aboard and operates accelerating the motion of the water mass in the U-duct. The theoretical analysis is conducted in the hypothesis of harmonic excitation and includes an equivalent linearization procedure for the turbulent air flow through the upper valve regulating the efflux from the one to the other tank. The application of the laws of thermodynamics to the open air system overhanging the water in each tank chamber reveals the negligibility of the heat transfer through the tank wall in comparison with the mass transfer effects. As a practical result, the mathematical model permits developing a suitable optimization process with the aim at the best damping operation, which however must be subjected to two fundamental constraints: the system stability and the pre-imposed limit power absorbable from the control equipment. Comparing with natural damped passive systems, a reduction of the order of 20–40% can be roughly attained for the resonant roll amplitude, depending on the supplied control power.



## 1. Introduction

Several anomalous motions may arise during the ship sailing through a rough sea, such as surge, heave and pitch in the vertical plane, sway and yaw in the horizontal one, roll around the longitudinal axis. The roll motion was not a problem all through the past sailer age, but became a serious trouble since the diffusion of the steam propulsion after the middle of the 19th century, due to its damping difficulty, particularly in the resonance range. The first anti-roll systems appeared in the warship construction, owing to the need of limiting the inconvenience caused by the roll to the cannon laying.

The stabilization of the rolling motion has challenged the marine engineers for more than one hundred years and is still the object of extensive researches of naval designers and architects (e.g., see Moaleji and Greig, 2007, for a survey over the history of anti-roll systems). Among the various solutions, three main types are classifiable, the fin or bilge keel arrangements, the gyro-stabilizers and the water tanks. The first ones are effective only for rather large cruising speeds, particularly in the case of adjustable slope ("active" fins), but are inefficacious for slow sailing and moreover, they are highly vulnerable; the gyroscopic systems benefited from a discrete diffusion in the first half of the 20th century, starting from some applications in heavy ships like the Italian liner *Conte di Savoia* (Krall, 1940), but were in part abandoned due to the requirement of concentrating large masses (hundreds of tonnes) in a restrict space inside the hold and to their malfunctioning for highly irregular wave motions; the water tanks were given up for a long period, but are becoming popular again nowadays.

The anti-roll damping tanks are characterized by a relative simplicity, an acceptable cost and a good efficacy for all sailing speeds. They were first devised by Froude (1861), were developed by Watts in their free-surface configuration (Watts, 1883, 1885), and then were improved by Frahm, who conceived the idea of the U-shape, splitting the reservoir in two parts with smaller free sloshing surfaces (Frahm, 1911). The concept is similar to the dynamic vibration absorber, where the role of the secondary mass is played by the water inside the tanks. This type of solution was first implemented in many German passenger or war ships, such as for example *Europa* and *Hamburg*.

In the following, other modifications of the Frahm conception were tried, as for example the free-flooding arrangement (Vasta et al., 1961), where the lower water duct had been removed and the tanks communicated directly with the sea, gaining the advantage of a simplification of the ship architecture, though their beneficial anti-roll effect was successful only for a limited speed-range.

* Corresponding author. Tel.: +39 91 2389 7283; fax: +39 91 2386 0672.
*E-mail address:* francesco.sorge@unipa.it (F. Sorge).

0029-8018/$ - see front matter © 2012 Elsevier Ltd. All rights reserved.
http://dx.doi.org/10.1016/j.oceaneng.2012.07.034

**Nomenclature**

$A_{charge/discharge}$ efflux area of control ports [$m^2$]
$B=2\gamma S_t b_t/V_e$ dimensionless volume variation parameter
$c_p$ and $c_v$ constant pressure and constant volume specific heats [$J\times kg^{-1}\times K^{-1}$]
$c_\theta$ and $c_\psi$ angular damping coefficients of roll motion and water motion [$N\times m\times s$]
$C_f$ dimensionless feed coefficient
$C_l$ and $C_t$ dimensionless coefficients of laminar and turbulent efflux through central valve $V_c$
$d_\theta=0.5c_\theta/\sqrt{k_sJ_s}$ and $d_\psi=0.5c_\psi/\sqrt{k_sJ_s}$ damping factors of roll motion and water motion
$g$ acceleration of gravity [$m/s^2$]
$G_c$ mass flow through central valve $V_c$ [$kg\times s^{-1}$]
$G_{charge/discharge}$ feeding/draining mass flows [$kg\times s^{-1}$]
$G_{in}$ and $G_{out}$ total air mass flows towards the inside and the outside of the tanks [$kg\times s^{-1}$]
$H=k_hS_h/(c_pM_e\omega_s)$ dimensionless heat transfer parameter
$I_1$, $I_2$ dimensionless duct-shape integrals
$J_1=J_{w1}/J_s$, $J_2=J_{w2}/J_s$ dimensionless moments of inertia of water
$J_s$ ship+water moment of inertia around longitudinal axis [$kg\times m^2$]
$J_w$ water moment of inertia with respect to vertical axis [$kg\times m^2$]
$J_{w1}=J_wI_1/2$, $J_{w2}=J_wI_2/2$ shape-corrected moments of inertia of water [$kg\times m^2$]
$k_h$ heat transfer coefficient [$J\times s^{-1}\times m^{-2}\times K^{-1}$]
$k_p$ air pressure restoring coefficient [$N\times m$]
$k_s=M_sgh_M$ sea buoyancy restoring coefficient [$N\times m$]
$k_w$ tank water restoring coefficient [$N\times m$]
$K_w=k_w/k_s$, $K_p=k_p/k_s$ dimensionless restoring parameters
$l$ abscissa along duct line [m]
$L$ Lagrangian function
$M_0=M_sgh_M\theta_0=k_s\theta_0$ amplitude of wave exciting moment [$N\times m$]
$M$ and $M_e$ air mass and equilibrium air mass inside tank [kg]
$M_s$ ship+water mass [kg]
$M_w$ tank water mass [kg]
$p_0$ feeding pressure inside supply reservoir [Pa]
$p_e=(p_p+p_s)/2$ equilibrium tank pressure [Pa]
$p_p$ and $p_s$ port and starboard tank pressure [Pa]
$P=(p_s-p_p)/p_e$ dimensionless pressure drop
$Q$ heat flux [$J\times s^{-1}$]
$r=\omega/\omega_s$ dimensionless frequency
$r_w=\omega_w/\omega_s$ water-to-ship frequency ratio
$R=c_p-c_v$ gas constant [$J\times kg^{-1}\times K^{-1}$]
$RH_j$ $j$th Routh–Hurwitz determinant
$S$ generic U-duct section [$m^2$], or else entropy [$J\times kg^{-1}\times K^{-1}$]
$S_h$ heat transfer surface [$m^2$]
$T$ temperature [K]
$U$ potential of conservative forces [$N\times m$]
$v$ specific volume [$m^3/kg$]
$V_e$ equilibrium air volume inside tank [$m^3$]
$\gamma=c_p/c_v$ isentropic exponent
$\delta_a$ and $\delta_w$ air density and water density [$kg/m^3$]
$\Delta=(T_s-T_p)/T_e$ dimensionless temperature drop
$\eta$ turbo-blower efficiency
$\theta_0$ wave slope
$\sigma=\omega_n/\omega_s$ characteristic number
$\tau=\omega t$ dimensionless time variable
$\omega_n$ system natural frequency [$s^{-1}$]
$\omega_s=\sqrt{k_s/J_s}$ roll natural frequency [$s^{-1}$]
$\omega_w=\sqrt{k_w/J_{w1}}$ water natural frequency [$s^{-1}$]

*Subscripts and superscripts*

$a$ air
atm atmospheric
$f$ control feed flow
$l$ laminar
$e$ equilibrium condition
$p$, $s$ port, starboard
$s$ ship
$t$ turbulent, or else tank
stagn stagnation conditions
$w$ tank water
$\dot{(\ldots)}$ derivative with respect to time $t$
$(\ldots)'$ derivative with respect to dimensionless time $\tau$
$\bar{(\ldots)}$ complex quantity

The main defect of all passive tank systems is the slowness of their response to the changes of the rolling angle. For this reason, many researchers have turned their attention to the active systems in the recent past, where the water motion is forced somehow from the one to the other tank by means of suitable pumping devices or other ingenious installations, with the collateral help of proper control equipments. The active working may be realized either directly through the displacement of the water mass (e.g., see Bell and Walker, 1966), or by opening and closing suitable control valves, for example located on the ceiling of the air chambers (van Daalen et al., 2000).

The theoretical modelling of such anti-roll systems has made large progresses after the appearance of high speed electronic calculators, permitting in particular the analysis of the flow three-dimensionality and the study of very complex control schemes. Starting from the first theoretical descriptions of the tank anti-roll systems (e.g., Krall, 1940), more and more advanced mathematical models have been proposed, including also the in-depth analysis of the auxiliary control systems (e.g., Moaleji and Greig, 2006; Marzouk and Nayfeh, 2008, 2009; Zhang et al., 2004; Holden, 2011), often being their only drawback the lack of a complete experimental validation on the sea, often very difficult to put into effect.

The present analysis focuses on an original air-activated U-tank system, based on a control criterion proportional to the water relative displacement, which is very simple to analyze and realize. Its characteristic principle is to help the displacement of the water mass from the tank that is emptying out towards the one that is filling by the proper push of the pressurized air insufflated by a suitable turbo-blower set on board. When modelling the system dynamics, the study of the physical evolution inside each chamber indicates that the heat transfer is negligible in practice in comparison with the effects of the air mass transfer, whence adiabatic conditions are applied.

The anti-roll arrangement may be next optimized provided that some fundamental constraints are respected, i.e., the observance of the stability limits and of a pre-imposed power level to be absorbed by the control activation. Choosing a multi-mode operative arrangement, where the control system is active only in a narrow resonant range to damp the highest amplitude oscillations and remains inactive otherwise, the present solution seems to be sufficiently inexpensive, to succeed in cutting the resonant peaks of the frequency response by an amount of 30% roughly and to

remain quite stable at the same time. Clearly, the turbo-blower set has to be regulated in order to deliver the requested flow with an acceptable efficiency and to stop working during the passive mode.

Control strategies of this kind have been proposed by other researchers in the more or less recent past, as reported in the literature, e.g., achieving the water displacement by various hydraulic pumping systems or regulating the air flux by the proper opening/closing of suitable gates, *etc.*, but all these strategies appear somehow different from the present technique as mainly regards the particular proportional conception of the control criterion, which looks indeed innovative.

## 2. Theoretical model

Refer to the list of symbols and to Fig. 1 for the notation throughout the text.

The pressure levels $p_s$ and $p_p$ inside the starboard and port chambers are different due to the air mass flow $G_c$ through the central valve $V_c$, but their mean value $(p_s+p_p)/2$ can be approximately equated to the equilibrium value $p_e$ in the hypothesis of small amplitude oscillations The air flow regime through $V_c$ should be realistically regarded as turbulent and $G_c$ should be assumed proportional to the square root of the pressure drop $|p_s-p_p|$. Nevertheless, the non-linearity of this flow regime will be here faced by an equivalent linearization technique, as specified later on. On the other hand, since just small changes are supposed for the system variables, all the geometrical non-linearities may be neglected in order to ultimately arrive at a linear formulation, which turns out to be very helpful for a quick analysis of the dynamical behaviour.

When the port and starboard valves $V_p$ and $V_s$ are closed, the operation of the anti-roll system is passive. During the active working on the contrary, such valves alternatively open their respective air chambers either to a higher pressure vessel, which is kept at room temperature and is fed by a suitable turbo-blower set (top pressure $p_0$), or to the external discharge (atmospheric pressure $p_{\mathrm{atm}}$). The opening law of the valves is assumed proportional to the relative displacement of the water mass in the tanks, i.e., to $\psi$, in such a way as to increase the air charging of the tank whence the water is flowing out and the air draining from the one where the water is flowing in. The requested proportionality of the air flows to $\psi$ is easily feasible by properly choosing the pressure ratios $p_0/p_e$ and $p_e/p_{\mathrm{atm}}$ and controlling the opening areas of the valve mouths, for example by means of link mechanisms connected with floating masses located inside the tanks. These results can be obtained even with low pressure drops, provided that the oscillations inside the two tanks are so small that the efflux pressure ratio through the valves $V_p$ and $V_s$ may be considered approximately constant.

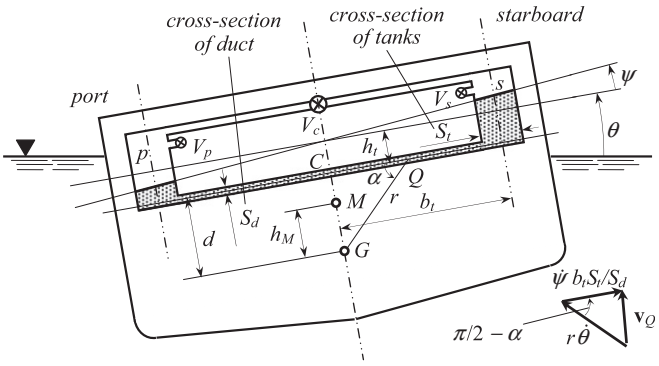


**Fig. 1.** Scheme of U-tank system ($M$: metacentre).

The water flow is assumed one-dimensional along the lower duct and the side tanks and the variable water configuration is identified by the instantaneous level inside the starboard tank $\psi(t)$. All physical quantities are assumed uniform inside each air chamber and their evolution is correlated to the temporal changes of the air volume and to the mass flow through the valves by a zero-dimensional thermodynamic model.

Considering an ideal rigid system formed by the ship plus the tank water centred and motionless with respect to the ship, indicate its mass with $M_s$ and its moment of inertia around the longitudinal axis with $J_s$. Moreover, indicate the water density with $\delta_w$, the water mass with $M_w$ ( $\cong 2\delta_w S_t h_t$), the moment of inertia of the water with respect to the central vertical axis with $J_w$ ( $\cong 2\delta_w S_t h_t b_t^2$) and the acceleration of gravity with $g$.

Defining then the area of the generic cross-section of the tank-duct tube with $S$, the square of the water absolute velocity at a generic location $Q$ is given by (Fig. 1)

$$v_Q^2 = r^2\dot{\theta}^2 + b_t^2\dot{\psi}^2\left(\frac{S_t}{S}\right)^2 - 2rb_t\dot{\theta}\dot{\psi}\left(\frac{S_t}{S}\right)\sin\alpha \tag{1}$$

where $\sin\alpha$ depends on the geometry of the U-tank system. For the scheme of Fig. 1, $\sin\alpha = d/r$ along the horizontal duct, while $\sin\alpha = -b_t/r$ along the tank axis. Eq. (1) permits calculating the total kinetic energy of the tank water, where the contribution of the first term at right hand just merges into the rotational kinetic energy $J_s\dot{\theta}^2/2$ of the whole ship.

In addition to the buoyancy restoring potential, $M_s g h_M \cos\theta$, also the gravitational potential associated with the tank water displacement must be taken into consideration. This potential is given by the difference of the potential of the water extra mass in the fuller tank minus the potential of the lacking water in the emptier tank. The total potential is found to be

$$U = M_s g h_M \cos\theta - \delta_w g S_t b_t^2 \tan\psi(\tan\psi\cos\theta + 2\sin\theta) \tag{2}$$

and introducing the auxiliary duct-shape integrals $I_1 = \int_s^p (S_t/S)(dl/h_t)$ and $I_2 = \int_s^p (r/b_t)\sin\alpha\,(dl/h_t)$, the Lagrangian of the water-ship system is

$$L = \frac{1}{2}\left[J_s\dot{\theta}^2 + \frac{J_w}{2}(I_1\dot{\psi}^2 - 2I_2\dot{\theta}\dot{\psi}) - M_s g h_M\theta^2 - M_w g\frac{b_t^2}{h_t}(\psi^2 + 2\psi\theta)\right] \tag{3}$$

Notice that $I_1 = 2[1+(b_t S_t)/(h_t S_d)]$ and $I_2 = 2(d/h_t - 1)$ for the scheme of Fig. 1.

We assume that the waves do not exert any resultant force on the hull but only an exciting moment, so that the ship mass centre $G$ does not move in the transverse plane. The roll forcing moment due to the waves is $M_s g h_M \theta_0 \sin\omega t = M_0 \sin\omega t$, where $\theta_0$ is the maximum wave slope, whose amplitude may be of a few degrees roughly, and $\omega$ is the exciting circular frequency. Moreover, some dissipative forces of the viscous type are supposed to act on the roll motion and on the water flux and the non-conservative moments $-c_\theta\dot{\theta}$ and $-c_\psi\dot{\psi}$ are introduced. Defining the dimensionless pressure drop $P = (p_s - p_p)/p_e$ and putting $J_{w1} = J_w I_1/2$, $J_{w2} = J_w I_2/2$, $k_s = M_s g h_M$, $k_w = M_w g b_t^2/h_t$, $k_p = S_t p_e b_t$ for brevity, the motion equations are

$$J_s\ddot{\theta} - J_{w2}\ddot{\psi} + c_\theta\dot{\theta} + k_s\theta + k_w\psi = M_0\sin\omega t \tag{4}$$

$$-J_{w2}\ddot{\theta} + J_{w1}\ddot{\psi} + c_\psi\dot{\psi} + k_w\theta + k_w\psi + k_p P = 0 \tag{5}$$

A thermodynamic relation, describing the evolution of the air mass overhanging the water inside each chamber, is needed for the closure of the mathematical problem, bearing in mind that the volume $V$ and the mass $M$ change because of the water motion and of the air flow through the valves.

Considering the air volume in each tank as an equipotential zero-dimensional open system, indicating the entering heat flux

with $Q$ and the air mass flows towards the inside and the outside with $G_{in}$ and $G_{out}$, the first law of thermodynamics may be written in the form

$$Q+c_p\left(\sum G_{in}T_{in,stagn}-\sum G_{out}T_{out,stagn}\right)=\frac{\gamma p\dot{V}+V\dot{p}}{\gamma-1} \tag{6}$$

where the subscript "stagn" refers to the stagnation conditions and $\gamma=c_p/c_v$ is the isentropic exponent.

In the hypothesis of small oscillations, it is legitimate to ascribe the equilibrium values $p_e$, $T_e$ and $V_e=v_eM_e$ to the pressure, temperature and volume of each air chamber and assume that the small changes affect only their derivatives, specifying however the heat flux in the form $Q=k_hS_h(T_{external}-T_{internal})$. Then, applying the perfect-gas law $pV=RTM$ to the air mass, where $R=c_p-c_v$ is the gas constant, Eq. (6) changes into

$$\frac{Rk_hS_h(T_{external}-T_{internal})}{c_pp_eV_e}+\left(\sum G_{in}\frac{T_{in,stagn}}{T_e}-\sum G_{out}\frac{T_{out,stagn}}{T_e}\right)\frac{1}{M_e}=\frac{\dot{p}}{\gamma p_e}+\frac{\dot{V}}{V_e} \tag{7}$$

while on the other hand, the equation of state gives also by differentiation

$$\frac{\dot{T}}{T_e}=\frac{\dot{p}}{p_e}+\frac{\dot{V}}{V_e}-\frac{\sum G_{in}-\sum G_{out}}{M_e} \tag{8}$$

It will be shown in the following that the air supply system has to be planned in such a way that the net air mass flows in the two tanks are equal and opposite. Then, specifying Eqs. (7) and (8) for each tank, i.e., replacing $p$, $T$ and $V$ first with $p_s$, $T_s$ and $V_s$ and then with $p_p$, $T_p$ and $V_p$, ignoring the differences among $T_{in,stagn}$, $T_{out,stagn}$ and $T_e$ because of the oscillation smallness, which mainly affects the flows $G_{in}$ and $G_{out}$ directly, subtracting the equations of the one and the other tank, we get after some algebra

$$\dot{\Delta}=\left(\frac{\gamma-1}{\gamma}\right)\dot{P}-H\omega_s\Delta \tag{9}$$

$$\dot{P}=B\dot{\psi}-2\gamma\frac{(\sum G_{in}-\sum G_{out})_p}{M_e}-\gamma H\omega_s\Delta \tag{10}$$

where $\Delta=(T_s-T_p)/T_e$, $B=2\gamma S_tb_t/V_e$, $H=k_hS_h/(c_pM_e\omega_s)$ and the ship natural frequency $\omega_s=\sqrt{k_s/J_s}$ was introduced.

It is to be expected, due mainly to the largeness of the tank volumes, that the dimensionless heat transfer parameter $H$ is quite small for this kind of application, whence the last term at right hand of Eq. (10) may be neglected with respect to the others, as if all evolutions were adiabatic and the relative temperature difference $\Delta$ were uncoupled with the other variables. More precisely, applying a perturbation procedure where the ratio $H\omega_s/\omega$ is the small perturbing parameter, the zero order temperature difference $\Delta^{(0)}$ appears proportional to the zero order pressure drop $P^{(0)}$ by Eq. (9) and the first order correction of the trinomial $\dot{P}-B\dot{\psi}+2\gamma(\Sigma G_{in}-\Sigma G_{out})_p/M_e$ due to the heat flux may be formally calculated by Eq. (10). Applying the second law of thermodynamics, $TdS=c_pdT-vdp$, one may arrive at the relation $(dS/c_v)=(dp/p)+\gamma(dV/V)+\gamma(dM/M)$, giving for the starboard and port chambers, respectively, and for the entropy difference between them

$$\frac{\dot{S}_s}{c_v}=\frac{\dot{p}_s}{p_e}-\frac{B\dot{\psi}}{2}-\gamma\frac{G_s}{M_e}\quad\frac{\dot{S}_p}{c_v}=\frac{\dot{p}_p}{p_e}+\frac{B\dot{\psi}}{2}-\gamma\frac{G_p}{M_e}\quad\frac{\dot{S}_s-\dot{S}_p}{c_v}=\dot{P}-B\dot{\psi}+2\gamma\frac{G_p}{M_e} \tag{11a, b, c}$$

because $p_s-p_e=p_e-p_p=(p_s-p_p)/2$, $\dot{p}_p=-\dot{p}_s$, $G_p=(\sum G_{in}-\sum G_{out})_p=-G_s=-(\sum G_{in}-\sum G_{out})_s$. Thus, the trinomial at right hand of Eq. (11a) is proportional to the time derivative of the entropy in the starboard chamber, which is in turn opposite to the homologous quantity of the port chamber by Eq. (11b), while their difference, given by Eq. (11c), is equal and opposite to the heat flux by Eq. (10). Therefore, the cyclic evolution inside each tank may be qualitatively represented in the temperature-entropy plane as in Fig. 2, where $E$ indicates the equilibrium point and the port and starboard conditions

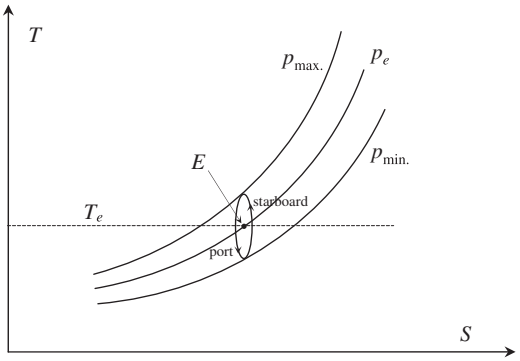


**Fig. 2.** Qualitative portrait on the temperature-entropy plane of the cyclic thermodynamic evolution of the air mass inside the tank chambers ($E$: equilibrium conditions). The cycle area is magnified for clarity reasons.

are out of phase of an angle $\pi$. For $H\to0$, the cycle width shrinks until becoming a vertical segment between the extreme isobars and this is roughly the actual situation.

Therefore, neglecting the heat flux, assuming in a first instance that the valves $V_s$ and $V_p$ are closed and the control system is inactive, Eq. (10) may be written as follows

$$\dot{P}=B\dot{\psi}-2\gamma\frac{G_c}{M_e} \tag{12}$$

In the hypothesis of a laminar efflux through the valve $V_c$, the mass flow $G_c$ is proportional to the pressure drop $P$ and the subtractive term at right hand of Eq. (12) may be written in the form $C_l\omega_sP$, where $C_l$ is a proper dimensionless laminar coefficient. As a turbulent efflux is most likely to occur, it is better to consider $G_c$ proportional to the square root of $P$ and write the third term of Eq. (12) in the turbulent form $C_t\omega_s|P|^{1/2}\mathrm{sgn}(P)$, where the dimensionless turbulent coefficient $C_t$ was introduced. For the laminar and turbulent cases we have thus, respectively

$$\dot{P}=B\dot{\psi}-C_l\omega_sP\quad\dot{P}=B\dot{\psi}-C_t\omega_s\sqrt{|P|}\,\mathrm{sgn}(P) \tag{13a, b}$$

The fifth order differential system, Eqs. (4), (5) and (13a) or (13b), points out two and a half degrees of freedom and has to be faced by numerical procedures in the turbulent non-linear case, Eq. (13b), starting for example from random initial values of the variables. Nevertheless, once reaching the steady conditions in a wide range of examined cases, the numerical solutions show nearly sinusoidal responses for $\theta$ and $\psi$, whereas the diagrams of $P$ may be well fitted by a function of the type $0.5\ P_{max.}(1-\cos2\omega t)\mathrm{sgn}(\sin\omega t)=P_{max}\sin^2\omega t\ \mathrm{sgn}(\sin\omega t)$, revealing the predominance of the first harmonic in the solution of the system equations (observe Fig. 3). Therefore, $\sqrt{|P|}\,\mathrm{sgn}(P)\cong\sqrt{P_{max.}}\sin\omega t$ and it is easy to apply an equivalent linearization procedure to simplify the analytical treatment of the problem. Here, the prescribed equivalence consists in imposing the same amplitude $P_{max.}$ to the linear approximation and in correlating the coefficients $C_t$ and $C_l$ so that the same amount of air mass is delivered during one single half cycle ($0<\omega t<\pi$) by both the non-linear and linear equivalent valves. This condition leads to the relation $C_t=C_l\sqrt{P_{max.}}$, which implies that, fixing $C_t$, the equivalent coefficient $C_l$ turns out to be a function of the frequency and amplitude of the wave excitation through the amplitude ratio $P_{max.}/\theta_0$, where $\theta_0=M_0/k_s$ may be considered as a "static" roll rotation.

Assuming in the second instance that the valves $V_s$ and $V_p$ are partially open and the control system is active, the mass flow $\dot{M}$ must take into consideration also the air charged or discharged through such valves and the control strategy governing this feeding. Let us suppose that this additional air flow is proportional to the relative displacement $\psi$ of the water mass and is positive in the one and negative in the other valve so as to

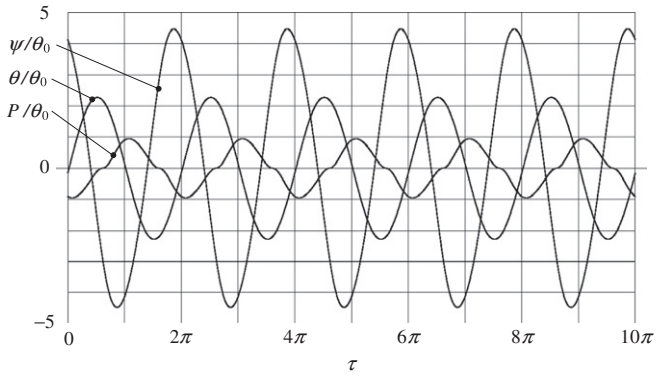


**Fig. 3.** Example of Euler–Cauchy numerical solutions for the case of non-linear efflux through valve $V_c$. Data: $J_1=0.05$, $J_2=0.0005$, $\omega_w/\omega_s=1.4$, $\omega/\omega_s=0.9$, $K_p/J_1=5$, $B=4, d_\theta=0.15$, $d_\psi=0.01$, $C_f=5$, $C_t/\sqrt{\theta_0}=27.426$ ($C_{l,\text{equivalent}}=30$), $C_{l,\text{laminar stability threshold}}=12.755$.

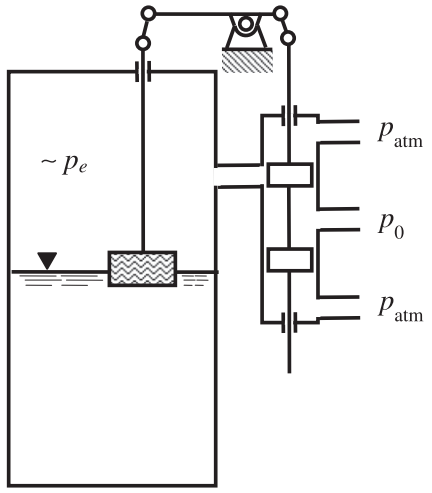


**Fig. 4.** Schematic description of pneumatic control system.

enhance the water displacement itself. This yields in practice the addition of two negative terms at right hands of Eq. (13a,b)

$$\dot{P}=B\dot{\psi}-C_l\omega_s P-C_f\omega_s\psi \quad \dot{P}=B\dot{\psi}-C_t\omega_s\sqrt{|P|}\,\mathrm{sgn}(P)-C_f\omega_s\psi \tag{14a, b}$$

where $C_f$ is a dimensionless feeding coefficient.

From a formal viewpoint, this strategy could be realized by simple floating devices like the one in Fig. 4, on condition that the flow through the distributing valve is proportional to its opening width, i.e., to $\psi$. This proportionality can be obtained even with small pressure ratios provided that the pressure oscillations inside the tanks are sufficiently small in comparison with the mean pressure $p_e$. Clearly, more sophisticated equipments are to be installed if the floating system is insufficient and some extra power is needed for the valve opening.

According with the efflux laws, the mass flows during the charge and discharge phases are

$$G_{\text{charge}}=\frac{cA_{\text{charge}}p_0}{\sqrt{RT_e}}\sqrt{\left(\frac{2\gamma}{\gamma-1}\right)\left[\left(\frac{p_e}{p_0}\right)^{(2/\gamma)}-\left(\frac{p_e}{p_0}\right)^{((\gamma+1)/\gamma)}\right]}$$

$$G_{\text{discharge}}=\frac{cA_{\text{discharge}}p_e}{\sqrt{RT_e}}\sqrt{\left(\frac{2\gamma}{\gamma-1}\right)\left[\left(\frac{p_{\text{atm}}}{p_e}\right)^{(2/\gamma)}-\left(\frac{p_{\text{atm}}}{p_e}\right)^{((\gamma+1)/\gamma)}\right]} \tag{15a, b}$$

where the same discharge coefficient $c$ is assumed for the two flows and the small differences among the temperatures are approximately neglected supposing that the higher pressure reservoir is refrigerated to the room temperature ($T_0\cong T_e$, $T_p\cong T_s\cong T_e$).

In order to not increase or decrease the total air mass inside the tanks in the long run, such mass flows may be made equal imposing that $A_{\text{charge}}\ p_0=A_{\text{discharge}}\ p_e$ and $p_e/p_0=p_{\text{atm}}/p_e$, which can be obtained for example by properly designing different angular widths of the charge and discharge openings in the distributing valve of Fig. 4. For example, when the water is emptying out from one of the two tanks, either at port or at starboard, the floating mass gets down, the distributing valve slides up and the air chamber is connected to the high pressure reservoir, whence the flow is proportional to the water surface displacement, i.e., to $\psi$, as conjectured above. Of course, a reverse evolution occurs in the other tank, which is being filled by the water. Since the heights of the openings are proportional to $\psi$, the whole effect may be represented by the third terms at right hand of Eq. (14 a,b).

According to the above assumptions, the mass flow $G_c$ must be replaced with $G_c+G_{\text{charge}}$ in Eq. (12) and moreover, comparing with Eq. (14), we get

$$C_f=\frac{2\gamma G_{\text{charge}}}{\omega_s M_e\psi} \tag{16}$$

where the ratio $G_{\text{charge}}/\psi$ is to be considered constant by Eq. (15), as $A_{\text{charge}}$ is proportional to $\psi$.

It must be noticed that the small pressure changes in the air chambers affect the air flows $G_{\text{charge}}$ and $G_{\text{discharge}}$ slightly, but in the same way, so that their sum remains null in practice, though the linear assumption of the law $G(\psi)$ becomes slightly weaker.

In addition, some device of the type in Fig. 5 has to be planned with the purpose of restoring the mean pressure $p_e=(p_s+p_p)/2$ in the tanks after some positive or negative occasional leakage. In this device, the two valves $V_{c,s}$ and $V_{c,p}$ are normally in series, playing as a whole the role of the single valve $V_c$ of Fig. 1. Yet, when for example the mean pressure decreases under its prefixed value, which is controlled by the spring load, the distributing valve slides upwards connecting both tanks with the higher pressure reservoir, as long as the desired mean pressure level is restored again.

In both devices, of Figs. 4 and 5, the space under the lower disc communicates with the external atmosphere and has just the purpose of balancing the forces acting on the slider.

## 3. Frequency response

The differential system, Eqs. (4), (5) and (14a), may be transformed into dimensionless form defining the new time

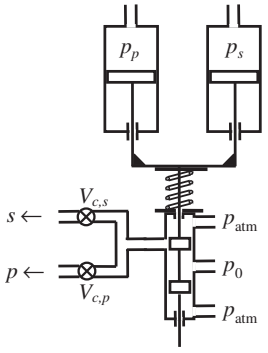


**Fig. 5.** Scheme of air pressure restoring device.

variable $\tau=\omega t$, indicating the differentiation with respect to $\tau$ with primes, whence $d(\dots)/dt=\omega(\dots)'$, *etc.*, and introducing the dimensionless parameters $r=\omega/\omega_s$ (exciting frequency), $r_w=\omega_w/\omega_s=(\sqrt{k_w/J_{w1}})/\omega_s$ (water frequency), $K_w=k_w/k_s$, $K_p=k_p/k_s$ (unit restoring moments), $J_1=J_{w1}/J_s$, $J_2=J_{w2}/J_s$ (moments of inertia), $d_\theta=0.5\ c_\theta/\sqrt{k_sJ_s}$, $d_\psi=0.5\ c_\psi/\sqrt{k_sJ_s}$ (damping factors):

$$r^2\theta''+2d_\theta r\theta'+\theta-J_2r^2\psi''+K_w\psi=\theta_0\sin\tau \tag{17}$$

$$-J_2r^2\theta''+K_w\theta+J_1r^2\psi''+2d_\psi r\psi'+K_w\psi+K_pP=0 \tag{18}$$

$$Br\psi'-C_f\psi-rP'-C_lP=0 \tag{19}$$

where one has just to replace $C_lP$ with $C_t\sqrt{|P|}\,\mathrm{sgn}(P)$ in Eq. (19) when the flow through the valve $V_c$ is considered turbulent, according to Eq. (14b)

Replacing $\sin\tau$ with $\exp(i\tau)$ at right hand of Eq. (17) and using the complex notation $\theta=\overline{\theta}_{\max.}\exp(i\tau)$, $\psi=\overline{\psi}_{\max.}\exp(i\tau)$, $P=\overline{P}_{\max.}\exp(i\tau)$, where the over-bars indicate complex amplitudes, one gets

$$\frac{\overline{\theta}_{\max.}}{\theta_0}=\frac{C_l(K_w-J_1r^2)-C_fK_p-2r^2d_\psi+ir(K_pB+K_w-J_1r^2+2C_ld_\psi)}{\overline{D}} \tag{20}$$

$$\frac{\overline{\psi}_{\max.}}{\theta_0}=-\frac{(K_w+J_2r^2)(C_l+ir)}{\overline{D}} \tag{21}$$

$$\frac{\overline{P}_{\max.}}{\theta_0}=\frac{(K_w+J_2r^2)(C_f-irB)}{\overline{D}} \tag{22}$$

where

$$\begin{aligned}\overline{D}=&(1-r^2)[C_l(K_w-J_1r^2)-C_fK_p]-C_l[(K_w+J_2r^2)^2+4d_\theta d_\psi r^2]+\\&-2r^2[d_\theta(K_pB+K_w-J_1r^2)+d_\psi(1-r^2)]+\\&+ir\Big\{(K_pB+K_w-J_1r^2)(1-r^2)-(K_w+J_2r^2)^2-4d_\theta d_\psi r^2+\\&+2C_ld_\psi(1-r^2)+2d_\theta[C_l(K_w-J_1r^2)-C_fK_p]\Big\}\end{aligned} \tag{23}$$

and the real amplitude ratios, $\theta_{\max.}/\theta_0$, $\psi_{\max.}/\theta_0$ and $P_{\max.}/\theta_0$, are given by the ratio of the moduli of Eqs. (20)–(22).

Fixing the wave amplitude $\theta_0$ and the turbulent coefficient $C_t$, the equivalent laminar coefficient $C_l$ must be calculated by trial and error for each dimensionless frequency $r$, updating Eq. (22) until $C_l\equiv C_t/\sqrt{P_{\max.}}$, so that the equivalent laminar valve delivers the same mass flow during each half-cycle, with the same pressure drop amplitude $P_{\max.}$.

Fig. 6 shows the parametric diagram of the frequency response of the angular roll, fixing the parameters $K_p$ and $C_f$ and all the other physical characteristics of the ship-anti-roll-system and varying the turbulent coefficient $C_t$. In practice, the data in the caption of Fig. 6 are sufficient to trace the frequency responses appearing in the figure, dividing the numerators and the denominators of Eqs. (20) and (22) by $J_1$ and accounting for the definitions reported in the list of symbols, whence $r_w^2=(\omega_w/\omega_s)^2=K_w/J_1$. For each point of the diagram, the equivalent laminar coefficient $C_l$ is first calculated by Eq. (22), through some iterative procedure aiming to satisfy the viscous-turbulent equivalence $C_l\equiv C_t/\sqrt{P_{\max.}}$, and then Eq. (20) yields the roll amplitude.

The highest resonant peak, over the top side of the figure, belongs to the response curve of the no-tank system. The sequence of the other plots shows first the full passive case ($C_f=C_t=0$) and then, fixing the flow coefficient ($C_f=5$), the efflux coefficient $C_t$ of the other cases is varied by steps until reaching a very large value (fully opened valve $V_c$). All the response curve are calculated on the basis of the equivalent laminar coefficient $C_l$, obtained by iterative procedures for each single point, as described above.

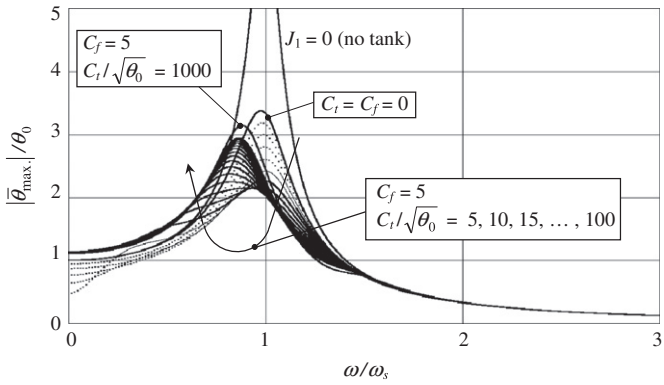


**Fig. 6.** Frequency response for various efflux coefficients $C_t$. Dots: unstable. Thick line: stable. Thin line: linear stability, non-linear instability. Data: $J_1=0.05$, $J_2=0.0005$, $\omega_w/\omega_s=1.4$, $K_p/J_1=10$, $B=4$, $d_\theta=0.15$, $d_\psi=0.01$.

As will be described in the following section, the stability analysis indicates that the inactive configuration with fully closed valve ($C_f=C_t=0$) is always stable, which is also intuitive, while different stability situations may show up in the other cases, depending also on the laminar or turbulent nature of the flow through the valve $V_c$. The parametric plots of Fig. 6 are drawn with dots and thick lines for the unstable and stable cases, respectively, whilst thin lines indicate fully stable conditions for the linear-laminar cases, but possible instability for the non-linear-turbulent cases. The non-linear stability must necessarily be checked by numerical integration and turns out to be a little weaker than the linear stability.

As shown in Fig. 6 and described in the following, the parameter $C_t$ may be optimized for the lowest resonance amplitude and this leads to quite appreciable results in the range from $r_w\cong1.2$ to $r_w\cong1.6$ roughly. Therefore, the diagrams of Fig. 6 were traced choosing a convenient in-between value of the water-to-ship frequency ratio $r_w$ ($=1.4$). Similarly, all other geometrical and physical parameters were preliminarily chosen within ranges consistent with verisimilar ship arrangements giving rise to the data in the caption. Moreover, realistic damping factors were ascribed to the external and internal damping, which subject the roll response to a natural attenuation even in the non-controlled mode, whence the beneficial effect of the active operation with respect to the pure undamped conditions is much larger. As regards the sensitiveness to the changes of these parameters, no remarkable modification of the speed responses may be appreciated by varying them in relatively large ranges and carrying out several numerical tests.

Comparing with some simple passive U-tank systems, where the external and internal damping suppresses the main resonance but generates two lower resonant peaks nearby, the present technique appears to smooth the frequency response more uniformly, attaining top values of $|\overline{\theta}_{\max.}/\theta_0|$ considerably lower than passive systems (e.g., see Moaleji and Greig, 2007, and Gaward et al., 2001).

Fig. 6 indicates that small and large turbulent flow coefficients $C_t$ produce relatively high peaks in the resonant range $\omega\cong\omega_s$, whereas a significant damping of the roll motion can be obtained choosing $C_t$ in a suitable intermediate range, where the motion appears also stable for its part: the peak amplitudes decrease first on increasing $C_t$, reach a minimum and then increase on increasing $C_t$ further. Furthermore, apart from this trend, observe that a remarkable advantage can be obtained in the low frequency range by opting for the inactive arrangement with fully closed valves ($C_f=C_t=0$).

These results suggest to choose a multi-mode planning of the anti-roll equipment, which exploits the damping properties of the active configuration in a narrow resonant range (active mode),

deactivating it and closing the control valves in the low and high frequency ranges (inactive modes). The values of the coefficients $C_f$ and $C_t$ for the active mode and the cross-over frequencies between the modes are to be calculated in advance by an optimization procedure in dependence on the overall system characteristics.

It is also noteworthy that Fig. 6 involves in practice some outlines of a sensitivity analysis of the control system, as the variation of the ship response due to the changes of the active air flow is clearly deducible by the diagrams. On the other hand, the response dependence on the other system data, which were prefixed in Fig. 6, can be verified to be very smooth carrying out more extensive numerical calculations.

Moreover, it is to be noticed that the system response to some possible irregular excitation can be easily derived by superposition procedures because of the linear structure of the theoretical model, including the non-periodic excitation, which may be dealt with by integral methods. This will be the subject of future developments of the present research. Nonetheless, some numerical tests with an irregular excitation of the type $\sum_{i=1,n} a_i \sin(\omega_i \tau/\omega + \varphi_i)$, where the $a_i$'s, $\omega_i$'s and $\varphi_i$'s are randomly chosen, show a stronger damping than the single harmonic excitation.

## 4. Stability

The autonomous solutions are obtainable in the linear case introducing the dimensionless characteristic number $\sigma = \omega_n/\omega_s$, where $\omega_n$ indicates a generic natural frequency, and putting $\theta = \hat{\theta}\exp(\sigma\tau/r)$, $\psi = \hat{\psi}\exp(\sigma\tau/r)$, $P = \hat{P}\exp(\sigma\tau/r)$ into Eqs. (4), (5) and (14a). The algebraic characteristic equation is of the fifth degree:

$$\begin{aligned}&(J_1 - J_2^2)\sigma^5 + [C_l(J_1 - J_2^2) + 2(d_\psi + J_1 d_\theta)]\sigma^4 \\ &+ [2C_l(d_\psi + J_1 d_\theta) + K_p B + K_w + J_1 + 2J_2 K_w + 4d_\theta d_\psi]\sigma^3 \\ &+ \{C_l(K_w + J_1 + 2J_2 K_w + 4d_\theta d_\psi) - C_f K_p + 2[d_\psi + d_\theta(K_w + K_p B)]\}\sigma^2 \\ &+ [2C_l(d_\psi + K_w d_\theta) + K_w - K_w^2 + K_p B - 2d_\theta C_f K_p]\sigma + [C_l(K_w - K_w^2) - C_f K_p] = 0\end{aligned} \tag{24}$$

When checking the stability of its roots by the Routh–Hurwitz method, the first four Routh–Hurwitz determinants $RH_j$ ($j = 1, 2, 3, 4$) are always found out positive in the field of interest of the various parameters. On the contrary, the fifth one is given by $[C_l(K_w - K_w^2) - C_f\ K_p] \times RH_4$ and reveals thus that the stability depends on the sign of the factor inside square brackets and increases on increasing the laminar coefficient $C_l$, as $K_w - K_w^2 > 0$, and on decreasing the feed coefficient $C_f$.

In the case of turbulent flux through the valve $V_c$, the system stability has to be checked by numerical integration of Eqs. (4), (5) and (14 b)) (e.g., by some Euler–Cauchy or Runge–Kutta routine), choosing and fixing the geometrical and physical parameters inside wide realistic ranges and starting the integration from random initial values of the system variables. Nevertheless, a fairly persistent feature observable from the results is that the linear stability conditions, given by Eq. (24), are worsened a little by the turbulent hypothesis, but this property always shows up in a somewhat regular way so that, as a heuristic rule of thumb, it is possible to assume that the stability limit is roughly reached in practice for a level of the equivalent laminar coefficient $C_{l,\mathrm{equivalent}}$ 1.5 times higher than the linear threshold. Respecting this limit, one can practically trust in the non-linear system stability with an excellent confidence.

## 5. Power absorption from the control system

According to Eq. (16), the total power spent during the active mode to supply compressed air, alternately to the one and the other tank, is given by

$$\begin{aligned}P_{\mathrm{control}} &= \frac{G_{\mathrm{blower}} p_{\mathrm{atm}}}{\eta \delta_{a,\mathrm{atm}}}\left(\frac{\gamma}{\gamma - 1}\right)\left[\left(\frac{p_0}{p_{\mathrm{atm}}}\right)^{((\gamma-1)/\gamma)} - 1\right] \\ &= \frac{\omega_s M_e p_{\mathrm{atm}}}{\pi \delta_{a,\mathrm{atm}}\, \eta(\gamma - 1)}\left[\left(\frac{p_0}{p_{\mathrm{atm}}}\right)^{((\gamma-1)/\gamma)} - 1\right] C_f\,|\overline{\psi}_{\mathrm{max.}}|\end{aligned} \tag{25}$$

where $G_{\mathrm{blower}} = G_{\mathrm{charge,max}} \int_0^\pi \sin\theta d\theta/\pi = 2G_{\mathrm{charge,max}}/\pi$ is the constant mass flow delivered by the turbo-blower into the supply reservoir, $\delta_{a,\mathrm{atm}}$ is the external air density and $\eta$ is the turbo-blower efficiency.

For a rough estimate, we can ascribe some realistic values to the various quantities appearing in Eq. (25), acceptable for example for a heavy passenger liner of 60,000 t. The mean air volume of each tank may be assumed of about 150 $m^3$, in the reasonable hypothesis that it is nearly equal to the underlying water volume, whose total mass is in turn supposed equal to 0.5% of the ship mass (300 t, including the two tanks and the duct). Typical values of the roll natural frequency and of the oscillation amplitude of the wave motion are $\omega_s = 0.45\ s^{-1}$ and $\theta_0 = 0.2$ rad, respectively, while the average value $\eta = 0.7$ may be ascribed to the compression efficiency. Using these numbers, one can roughly estimate that $P_{\mathrm{control,max.}} \cong 100 \times C_f\,|\overline{\psi}_{\mathrm{max.}}/\theta_0|$ kW for a compression ratio $p_0/p_{\mathrm{atm}} = 1.25$.

The mass flow required for the active operation may be provided by a few appropriate turbo-blower units working in parallel, for example to be chosen in the market in the top category delivering air flows larger than 100 $m^3/s$.

Of course, the blowing machines must be stopped during the passive operation and must be regulated so as to deliver the air flow in the best efficiency conditions during the active one. This regulation may be carried out for example by varying the number of active compression units, or the single compressor speeds, or the angles of attack of the blades, or even throttling the feeding pipes.

Comparing the power request by the pneumatic and hydraulic control systems, one has to impose the same water flow $G_{\mathrm{charge}}\delta_w/\delta_{a,e}$ between the tanks, in order to get equivalent damping effects. The total head of the hydraulic system is given by the sum of velocity, acceleration, elevation and pressure heads between the two chambers, which quantities are all variable but relatively small. As a rough approximation, the total head is of the order of magnitude of the product of the wave slope $\theta_0$, some fraction of one radian, and the factor $2gb_t$, so that, considering that the density ratio $\delta_w/\delta_{a,e}$ is usually not so far from 700 or thereabouts, the smallness of the head turns out to be compensated by the largeness of $\delta_w/\delta_{a,e}$ and the hydraulic pump device appears subject to nearly the same working task as the turbo-blower set.

Many active control systems have been proposed in the last years, whose feedback towards the pumping equipment may be of the proportional, integral or derivative type, or may even be adaptive, requiring some prediction of the control action to be applied. Taking into account the different weights and sizes of the installations examined by the various researchers and the other operative conditions, the results of the present model range approximately with the others, with regard to both the roll attenuation and the power consumption, but have the characteristic to be generated by a very simple, effective and "natural" control conception. Moreover, a certainly non-marginal advantage of the pneumatic arrangement with respect to the hydraulic one consists in the total absence of machines working inside the sea water and in the consequent easier maintenance of the dry equipment.

## 6. Optimization

An efficient optimization process should always respect two fundamental constraints: a sufficiently large level of the turbulent flow coefficient $C_t$, such that the equivalent laminar coefficient $C_l$ is at least one and a half times the stability threshold calculable as described previously; a sufficiently low feed control coefficient $C_f$, such that the power requested for the control device is kept below a pre-fixed desired level. It is to be said that the curtailment of this fraction of the ship propulsion power, to be transferred to the activation of the pneumatic control system, should not be considered in practice a serious drawback when sailing in a rough sea, where the full-speed cruising is seldom requested. Moreover, such a power request arises only near the resonant condition.

In the hypothesis of a multi-mode arrangement, the optimization must be done according to a procedure of the following type, repeating iteratively the step sequence used for Fig. 6: choose a convenient value of the water-ship frequency ratio $r_w$ (good results are obtained for $r_w=1.2$ to 1.6) start from some initial values of $C_f$ and $C_t$, for example very small; search the intersections of the active frequency response, whose parameters $C_f$ and $C_t$ are to be optimized, with the inactive plots where $C_f=0$ and $C_t$ is either null or optimized for its part; calculate the peak amplitude inside the frequency range between such intersections, where the active operation can indeed produce some benefit with respect to the passive conditions; vary $C_f$ and $C_t$ by trial steps while repeating the same operations, with the aim at minimizing the maximum amplitude. In order to trace the diagrams that follow, this procedure was properly transferred into the formulation of a numerical optimization code.

Fig. 7 shows the results of the optimization process for a three-mode example case. The optimum values of $C_f$ and $C_t$ were obtained by the above trial-and-error approach, increasing them separately stepwise until coming down to the minimum peak value throughout the frequency range. This optimization procedure considered the two constraints of the system stability and of the maximum pre-fixed power for the active operation. The zero power case $C_f=0$ (curve 0), which is passive as well, was only optimized as regards the opening of the central valve $V_c$.

Since all the curves numbered from 0 to 5 ($C_t>0$) tend to run closer and closer to each other on increasing the frequency above the ship own resonance ($\omega>\omega_s$), the over-resonance intersections among these curves are not easily identifiable in the figure, differently from their low frequency intersections with the curve $C_f=C_t=0$. Therefore, it is convenient to turn to the optimized inactive mode 0 just a little above the resonance and maintain this condition throughout the remaining high frequency range, preferring thus the passive anti-roll operation, which is totally free of charge. On the other hand, it is better to turn to the more convenient mode $C_f=C_t=0$ in the low frequency range.

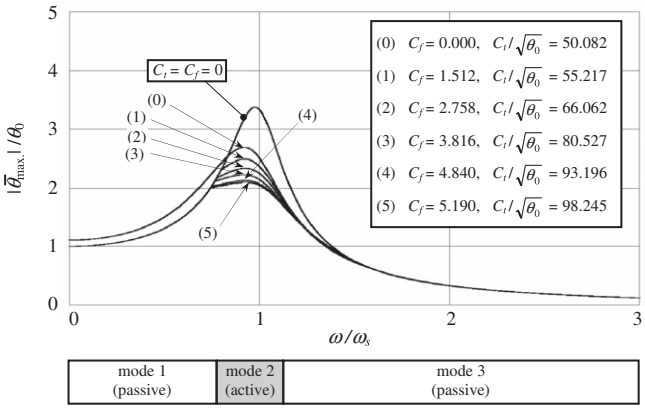


**Fig. 7.** Three-mode optimized frequency response ($P_{control}=100\,C_f|\overline{\psi}_{max.}/\theta_0|$). Curve 0: $C_f=0$, $P_{control}=0$, Curves (1) to (5) are subject to the respective constraints:, $C_f|\overline{\psi}_{max.}/\theta_0| \le$ 5, 10, 15, 20, 21 $\rightarrow P_{control} \le$ 500, 1000, 1500, 2000, 2100 kW, Mode 1 ($C_f=C_t=0$, passive): low frequency range; mode 2 ($C_f$ and $C_t$ optimized, active): resonant frequency range (curves 1 to 5); mode 3 ($C_f=0$ and $C_t$ optimized, passive): high frequency range (curve 0), Data: $J_1=0.05$, $J_2=0.0005$, $\omega_w/\omega_s=1.4$, $K_p/J_1=60$, $B=4$, $d_\theta=0.15$, $d_\psi=0.01$.

A particular feature verifiable in the whole range of interest of the parameters is that the best control of the amplitude is nearly always obtainable by applying the full level fixed for the admissible control power, unless this power begins to become large, in which case the roll amplitudes tend to decrease less and less and the stability constraint becomes prevalent. Therefore, the optimization process has just to be performed in practice on the efflux coefficient $C_t$ for the usual low levels of the admissible power, while the inopportuneness clearly appears of increasing too much the control power in the region where the growth of the attenuation gain becomes smaller and smaller, in order also to avoid too large oscillations of the water mass. Therefore, the highest power levels reported in Fig. 7 are to be considered as "asymptotic" and are never to be reached in practice.

The inactive closed-valve response ($C_f=C_t=0$) and the optimized inactive case ($C_f=0$, $C_t=$optimum) are reported in full. These modes are to be chosen in the low and high frequency ranges, respectively, whereas the control activation is limited to a narrow range around the resonance. As observable, the three-mode operation, characterized by the partial range active control conception, reduces the response peaks significantly with respect to the inactive cases, down by an amount of 20–40% roughly, depending on the control power used, which number becomes much higher when comparing with the pure undamped system. In the resonant sub-range the fraction of the total power absorbed by the active control may be estimated as quite less than 5% roughly, depending on the desired attenuation level. These may be considered as very good and not so much expensive results, minding the great advantages of achieving either better comfort conditions in the passenger liners or smoother goods shaking in the container ships.

## 7. Conclusion

An interesting U-tank equipment for the damping of the heavy ship roll motion by a convenient three-mode operation has been here conceived and analyzed from a theoretical point of view. Two modes are passive and operate in the small and high frequency ranges of the wave disturbance, while the third one is active, operates in a narrow neighbourhood of the resonant frequency and consists in practice in a pneumatic forcing of the water transfer from the one to the other tank, proportional to the water displacement itself.

Applying a harmonic wave excitation, an optimization procedure can be devised to minimize the amplitude peaks of the active mode by properly choosing the efflux and charge/discharge coefficients through the feeding valves. This procedure must be carried out by an iterative way, taking also into consideration two fundamental constraints: the limit threshold of stability and the pre-fixed level to be not exceeded by the power absorption from the pneumatic control system. This optimization process leads to a reduction of the roll amplitude by an amount of 20–40% roughly.

## References

Bell, J., Walker, P., 1966. Activated and passive controlled fluid tank system for ship stabilization. Trans. - Soc. Nav. Archit. Mar. Eng. 74, 150.

Frahm, H., 1911. Results of trails of the anti-rolling tanks at sea. Trans.Inst. Naval Archit. 53, 183.
Froude, W., 1861. On the rolling of ships. Trans.Inst. Naval Archit. 2, 180.
Gaward, A.F.A., Ragab, S.A., Nayfeh, A.H., Mook, D.T., 2001. Roll stabilization by anti-roll passive tanks. Ocean Eng. 28, 457–469.
Holden, C., Modelling and Control of Parametric Roll Resonance, Ph.D. Thesis, Norwegian University of Science and Technology, Department of Engineering Cybernetics, Trondheim, Norway, 2011.
Krall, G., 1940. Meccanica Tecnica delle Vibrazioni (in Italian). Zanichelli I, 268–290.
Marzouk, O.A., Nayfeh, A.H., A parametric study and optimization of ship-stabilization systems, 1st WSEAS International Conference on Maritime and Naval Science and Engineering (MN'08), Malta, September 11–13, 2008.
Marzouk, O.A., Nayfeh, A.H., 2009. Control of ship roll using passive and active anti-roll tanks. Ocean Eng. 36, 661–671.
Moaleji, R., Greig, A.R., Inverse Control for Roll Stabilization of Ships Using Active Tanks, MCMC, September 2006, Lisbon.
Moaleji, R., Greig, A.R., 2007. On the development of ship anti-roll tanks. Ocean Eng. 34, 103–121.
van Daalen, E.F.G., Kleefsman, K.M.T., Gerrits, J., Luth, H.R., Veldman, A.E.P., Anti-roll tank simulations with a volume of fluid (VOF) based Navier–Stokes solver, 23rd Symposium on Naval Thermodynamics, Valde Reuil, France, September 17–22, 2000.
Vasta, J., Gidding, A.J., Taplin, A., Stilwell, J.J., 1961. Roll stabilization by means of passive tanks. Trans. - Soc. Nav. Archit. Mar. Eng. 69, 411.
Watts, P., 1883. On a method for reducing the rolling of ships at sea. Trans. Inst. Naval Archit. 24, 165.
Watts, P., 1885. The use of water chambers for reducing the rolling of ships at sea. Trans.Inst. Naval Archit. 26, 30.
Zhang, H., Jiang, D., Liang, L., Huang, S., and Li, G., Modelling and simulation of passively controlled anti-rolling tank, Proceedings of the 5th World Congress on Intelligent Control and Automation, June 15–19, 2004, Hangzhou, P.R. China.